Provided for non-commercial research and education use.
Not for reproduction, distribution or commercial use.

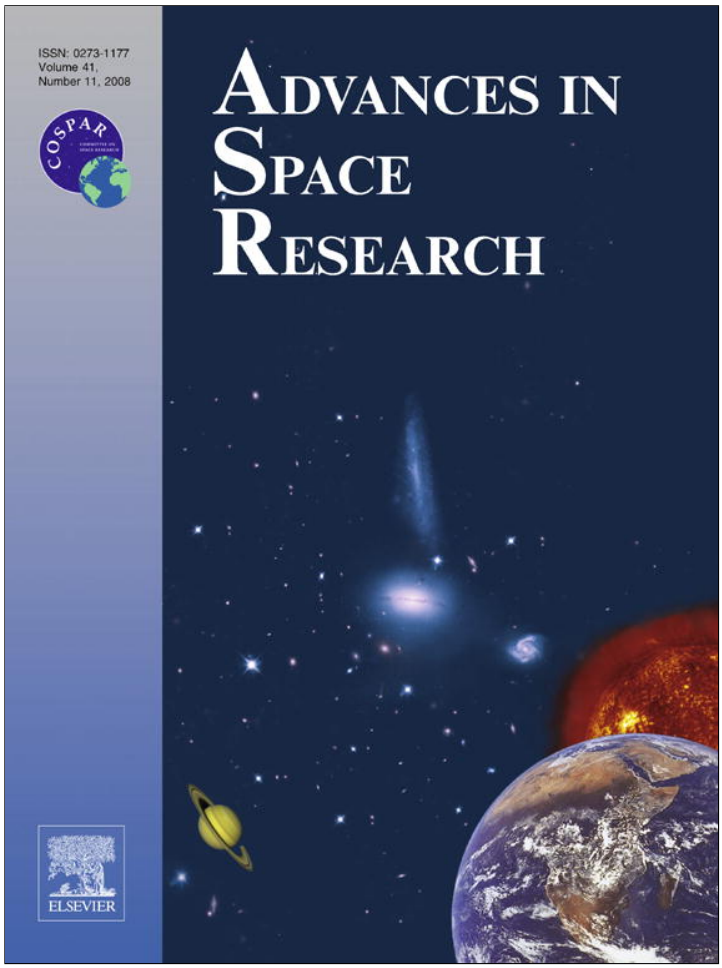

This article appeared in a journal published by Elsevier. The attached copy is furnished to the author for internal non-commercial research and education use, including for instruction at the authors institution and sharing with colleagues.

Other uses, including reproduction and distribution, or selling or licensing copies, or posting to personal, institutional or third party websites are prohibited.

In most cases authors are permitted to post their version of the article (e.g. in Word or Tex form) to their personal website or institutional repository. Authors requiring further information regarding Elsevier's archiving and manuscript policies are encouraged to visit:

http://www.elsevier.com/copyright

Author's personal copy

Available online at www.sciencedirect.com
ScienceDirect
Advances in Space Research 41 (2008) 1906–1913
ADVANCES IN SPACE RESEARCH (a COSPAR publication)
www.elsevier.com/locate/asr

The Geostationary Earth Radiation Budget Edition 1 data processing algorithms

S. Dewitte *, L. Gonzalez, N. Clerbaux, A. Ipe, C. Bertrand, B. De Paepe

Royal Meteorological Institute of Belgium, Ringlaan 3, B-1180 Brussels, Belgium

Received 18 October 2006; received in revised form 25 July 2007; accepted 27 July 2007

Abstract

The Geostationary Earth Radiation Budget (GERB) instrument is the first to measure the earth radiation budget from a geostationary orbit. This allows a full sampling of the diurnal cycle of radiation and clouds – which is important for climate studies, as well as detailed process studies, e.g. the lifecycle of clouds or particular aerosol events such as desert storms. GERB data is now for the first time released as Edition 1 data for public scientific use. In this paper we summarise the algorithms used for the Edition 1 GERB data processing and the main validation results. Based on the comparison with the independent CERES instrument, the Edition 1 GERB accuracy is 5% for the reflected solar radiances and 2% for the emitted thermal radiances.
© 2007 COSPAR. Published by Elsevier Ltd. All rights reserved.

Keywords: Earth Radiation Budget; Geostationary

1. Introduction

The climate on earth is determined by the radiative energy exchange at the top of the atmosphere. Averaged globally, the heating by incoming solar radiation has to be compensated by cooling by reflected solar radiation and emitted thermal radiation in order to have a stable climate. The spatial distribution of the net radiative energy gain of the earth drives the general circulation of the atmosphere and the oceans. In general net radiative energy is gained at warm locations, e.g. the equator with high solar incidence or clear sky regions with low albedo, and lost at cold locations, e.g. the poles with low solar incidence or cloud tops with high albedo. Thus the earth satisfies the basic conditions of a heat engine converting thermal into kinetic energy.

Earth Radiation Budget (ERB) measurements started from polar or low earth orbit satellites, e.g. with the Earth Radiation Budget Experiment (ERBE) (Barkstrom, 1984), the Scanner for Radiation Budget (ScaRaB) (Kandel et al., 1998) and the Cloud's and the Earth's Radiant Energy System (CERES) (Wielicki et al., 1996). Polar satellites have the advantage of global coverage, but the disadvantage of limited temporal sampling with only two measurements per day at midlatitude and equatorial regions. Thus they undersample the rapid variations of the local radiation budget, primarily due to the presence, motion and lifecycle of clouds, which have a strong influence on the radiation budget due to their high reflection and low temperature compared with clear sky conditions. Complementary to the polar radiation budget instruments, the first Geostationary Earth Radiation Budget (GERB) instrument was launched on the European Meteosat 8 satellite in August 2002. GERB makes measurements of the radiation budget every 6 min tracking as a function of time *individual* clouds or aerosol events such as desert storms, instead of using the *statistical* diurnal cycle approach needed with polar sampling.

The main steps in the GERB data processing are inherited from the polar radiation budget instruments. They are: radiance calibration, conversion of the measured spectrally broadband radiances to the exact spectral integrals of

* Corresponding author.
E-mail address: steven.dewitte@oma.be (S. Dewitte).
URL: http://gerb.oma.be (S. Dewitte).

0273-1177/$34.00 © 2007 COSPAR. Published by Elsevier Ltd. All rights reserved.
doi:10.1016/j.asr.2007.07.042

Author's personal copy

reflected solar radiation and emitted thermal radiation, and the conversion from the measured radiance in a single direction to a radiative energy flux. GERB and the multispectral high resolution Spinning Enhanced Visible and InfraRed Imager (SEVIRI) (Schmetz et al., 2002) are two instruments on board of the same satellite. We use SEVIRI as auxiliary instrument for the GERB data processing. SEVIRI is used both for scene identification within the GERB footprint as well as for resolution enhancement of the GERB products.

The first GERB data was obtained in December 2002. Since then GERB data has continuously been processed in near-real time, and the quality of the products has been assessed and improved. A second GERB instrument was launched on Meteosat 9 in December 2005. The GERB instruments have been launched in a different order than they were built, therefore GERB on Meteosat 8 is referred to as 'GERB 2' and GERB on Meteosat 9 is referred to as 'GERB 1'. At the launch of GERB 1 it was decided to freeze the processing software for GERB 2 and to release GERB 2 data for scientific usage. The near-real time data is referred to as 'Version 3' (V3). After a 40 day period for manual quality control the V3 is renamed 'Edition 1' (E1) and is made available in a long term archive.

This paper gives a summary of the GERB data processing performed at the Royal Meteorological Institute of Belgium (RMIB), referred to as 'RMIB GERB Processing' (RGP). Section 2 gives an overview of the RGP, describing the required processing steps and the division into subsystems. Section 3 describes the individual subsystems in more detail. Section 4 provides some validation results. Section 5 contains the conclusions.

2. Processing overview

2.1. Required processing steps

The estimation of reflected solar and emitted thermal fluxes from single satellite broadband radiance measurements has been done previously for the ERBE, ScaRaB and CERES missions. The experience from these experiments learns that the following steps are required to process GERB data:

- The calibration of the broadband radiances (Harries, 2004). A 'total' (TOT) radiance L_{TOT} is measured in the spectral range 0.3–100 μm and a 'shortwave' (SW) radiance L_{SW} is measured in the spectral range 0.3–4 μm.

$$L_{\mathrm{TOT}} = \int \Phi_{\mathrm{TOT}}(\lambda) L(\lambda) \mathrm{d}\lambda \qquad L_{\mathrm{SW}} = \int \Phi_{\mathrm{SW}}(\lambda) L(\lambda) \mathrm{d}\lambda \tag{1}$$

  $L(\lambda)$ is the spectral distribution of the observed radiation. The measured radiances (left side Eq. (1)) are referred to as filtered radiances L_{f} as they are filtered by the instrument spectral responses $\Phi_{\mathrm{TOT}}(\lambda)$ and $\Phi_{\mathrm{SW}}(\lambda)$.
- The coarse separation of the reflected solar and the emitted thermal radiances. For earth scenes $L(\lambda)$ has a contribution of reflected solar radiation $L_{\mathrm{sol}}(\lambda)$ and of emitted thermal radiation $L_{\mathrm{th}}(\lambda)$. $L_{\mathrm{sol}}(\lambda)$ has most of its energy below 4 μm and $L_{\mathrm{th}}(\lambda)$ has most of its energy above 4 μm. A synthetic 'longwave' (LW) radiance is computed by subtraction of the shortwave from the total radiance according to the following equation

$$L_{\mathrm{LW}} = L_{\mathrm{TOT}} - A L_{\mathrm{SW}} = \int (\Phi_{\mathrm{TOT}}(\lambda) - A \Phi_{\mathrm{SW}}(\lambda)) L(\lambda) \mathrm{d}\lambda \tag{2}$$

  The factor A is defined such that L_{LW} is zero when a black body of 5800 K (close to the solar spectrum) is observed. For earth scenes, there will be a small contribution of the reflected solar radiation $L_{\mathrm{sol}}(\lambda)$ to the synthetic LW radiance L_{LW} and a small contribution of emitted thermal radiation $L_{\mathrm{th}}(\lambda)$ to the SW radiance L_{SW}.
- The estimation of the spectral integrals of the reflected solar radiation L_{sol} and of the emitted thermal radiation L_{th}.

$$L_{\mathrm{sol}} = \int L_{\mathrm{sol}}(\lambda) \mathrm{d}\lambda \qquad L_{\mathrm{th}} = \int L_{\mathrm{th}}(\lambda) \mathrm{d}\lambda \tag{3}$$

  As L_{sol} and L_{th} are not filtered by a spectral response (compare Eq. (3) to Eq. (1)) they are referred to as unfiltered radiances L_{uf}. The unfiltered radiances L_{uf} are estimated from the filtered radiances L_{f} by multiplication with the unfilter factor $\alpha_{\mathrm{uf}} = L_{\mathrm{uf}}/L_{\mathrm{f}}$. This implements both a fine separation of the reflected solar and the emitted thermal radiances and a removal of the non flat spectral responses of the SW and the synthetic LW channel. Determination of α_{uf} involves a modelling of the spectral distribution of the observed radiation.
- The estimation of the fluxes from the observed radiances. This involves the modelling of the angular distribution of the observed radiation. This results in the estimation of a flux F. The ratio F/L_{uf} is referred to as the angular conversion factor or Angular Dependency Model (ADM). For the processing of SW GERB data we use the empirical ADM's derived from the CERES instrument on the Tropical Rainfall Measurement Mission (TRMM) satellite, using the Visible and InfraRed Scanner (VIRS) imager for scene identification (Loeb et al., 2003). For the processing of LW GERB data we use theoretical ADM's calculated using radiative transfer calculations (Clerbaux et al., 2003).

2.2. Unfilter and angular conversion methodology

Maximally accurate unfiltered radiance and flux estimates are obtained from a combination of GERB and SEVIRI data. GERB provides accurate broadband mea-

Author's personal copy

surements. SEVIRI provides multispectral information, which is useful for the unfiltering, and robust scene identification, which forms a necessary condition for the appropriate ADM selection. A rational way to obtain the best combined estimate of the unfiltered radiance L_{uf} and of the broadband flux F is given by the following equations

$$L_{uf} = \frac{L_{uf}^{SEV} L_f}{L_f^{SEV}} = C L_{uf}^{SEV} = \alpha_{uf} L_f \quad (4)$$

$$F = \frac{F^{SEV} L_f}{L_f^{SEV}} = C F^{SEV} = \alpha_{adm} \alpha_{uf} L_f \quad (5)$$

L_f is the basic filtered broad band GERB radiance (SW or synthetic LW) measurement. L_f^{SEV} is the estimate of the filtered broadband GERB radiance measurement, estimated from the SEVIRI spectral radiances only. L_{uf}^{SEV} is the corresponding estimate of the unfiltered broad band radiance, estimated from the SEVIRI spectral radiances only. F^{SEV} is the corresponding estimate of the unfiltered broadband flux, estimated from the SEVIRI spectral radiances only.

Eqs. (4) and (5) can be interpreted in two ways, which are strictly equivalent:

(1) The GERB broad band radiance measurement L_f is converted to a broad band unfiltered radiance by multiplication with the SEVIRI derived unfiltering factor $\alpha_{uf} = L_{uf}^{SEV}/L_f^{SEV}$. The obtained unfiltered radiance L_{uf} is further converted to the broadband flux by multiplication with the SEVIRI derived angular conversion factor $\alpha_{adm} = F^{SEV}/L_{uf}^{SEV}$.

(2) The SEVIRI estimated unfiltered radiance L_{uf}^{SEV} and broadband flux F^{SEV} are corrected by the factor $C = L_f/L_f^{SEV}$, which corrects the SEVIRI based spectral modelling by the GERB measurement.

2.3. Division into subsystems

An overview of the RGP is given in Fig. 1. It consists in total of three main subsystems: 'SEVIRI Processing', 'GERB Processing' and 'Resolution Enhancement', and of three types of averaging to produce output products in different space time resolutions, referred to as 'Averaged Rectified Geolocated' (ARG), 'Standard High resolution Image' (SHI) and 'Binned Averaged Rectified Geolocated' (BARG).

The subsystem 'SEVIRI Processing' has as input full resolution SEVIRI spectrally narrowband radiances – with 15′ sampling and 3 km nadir resolution – and as output 3×3 SEVIRI pixel resolution filtered radiance estimates and broadband unfiltered radiance and flux estimates. Those outputs are referred to as 'GERB-like products'. They have 15′ sampling and 9 km resolution at nadir. Within the SEVIRI Processing the unfilter factor α_{uf} and the angular conversion factor α_{adm} are modelled.

The subsystem 'GERB Processing' has as input the GERB measured filtered broadband radiances – present in the Non Averaged Non Rectified Geolocated (NANRG) product – as well as the GERB-like products, and as output GERB broadband unfiltered radiances and fluxes, with

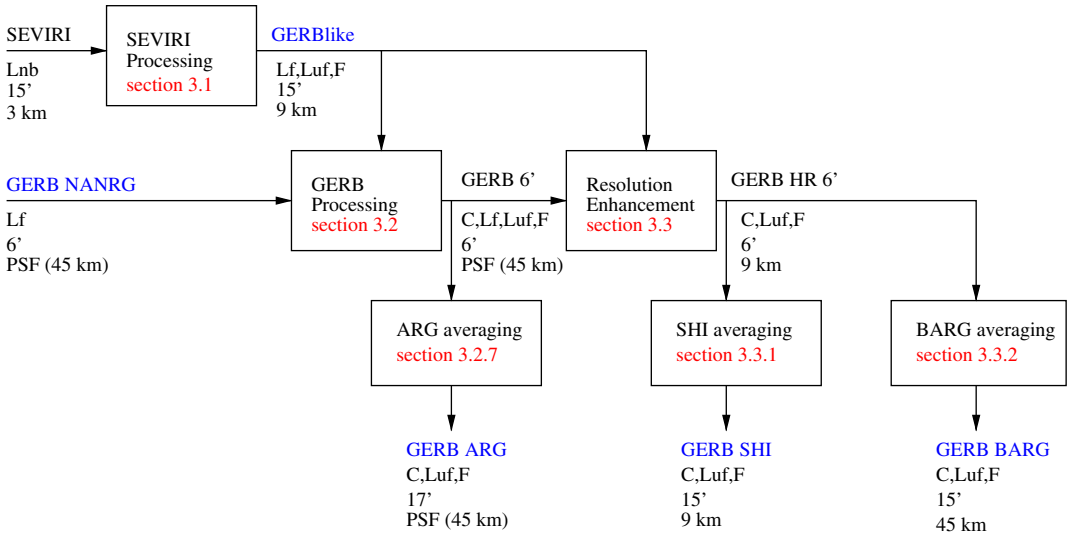

Fig. 1. RGP overview. Processing subsystems are indicated by boxes. For the input/output products next to the arrows, the following characteristics are given: name of the product (in blue if it is a GERB product available to an external user), main radiometric parameters contained in the product (L_{nb}: narrowband radiance, L_f: filtered radiance, L_{uf}: unfiltered radiance, F: flux, C: spectral correction factor), time resolution, spatial resolution (at nadir). For each subsection, the relevant section of this paper is indicated in red. Used acronyms: SEVIRI, Spinning Enhanced Visible and Infrared Imager; GERB, Geostationary Earth Radiation Budget; NANRG, Non Averaged Non Rectified Geolocated; ARG, Averaged Rectified Geolocated; SHI, Standard High resolution Image; BARG, Binned Averaged Rectified Geolocated; HR, High Resolution; PSF, Point Spread Function. (For interpretation of the references to colour in this figure legend, the reader is referred to the web version of this article.)

Author's personal copy

6′ sampling and GERB footprint (approximatively 45 km at nadir) resolution. Those outputs are referred to as 'GERB 6′ products'. Within the GERB Processing the Eqs. (2), (4) and (5) are applied.

The subsystem 'Resolution enhancement' has as input the GERB 6′ products and the GERB-like products. The high resolution of the GERB-like products is used to increase the resolution of the GERB 6′ products towards GERB High Resolution 6′ Products with a resolution of 9 km at nadir.

Three types of space time averaging are carried out to obtain three different product types:

- The ARG is the most basic product type with GERB footprint resolution, 17′ sampling and with minimal use of SEVIRI data;
- The SHI is the high resolution product with 3×3 SEVIRI sampling;
- The BARG is the binned version of the ARG, defined over precise space/time boxes, with 15′ sampling and 45 km at nadir.

In the following sections a brief description of the function of each of the subsystems is given.

3. Processing subsystems

3.1. SEVIRI Processing

In this subsystem the spectral modelling, as well as the scene identification and the associated angular modelling are done on the basis of SEVIRI data.

The inputs for this subsystem are the SEVIRI images of multispectral (narrowband) images. SEVIRI makes images of the earth at the wavelengths of 0.6, 0.8, 1.6, 3.9, 6.2, 7.3, 9.7, 10.8, 12 and 13.4 μm. The spatial resolution at nadir is 3 km. The sampling period is 15 min.

3.1.1. Spectral modelling

The spectral modelling consists in obtaining the estimate of the broadband filtered radiance $L_{\mathrm{f}}^{\mathrm{SEV}}(x_{\mathrm{S}}, y_{\mathrm{S}}, t_{\mathrm{S}})$ and of the unfilter factor $L_{\mathrm{uf}}^{\mathrm{SEV}}(x_{\mathrm{S}}, y_{\mathrm{S}}, t_{\mathrm{S}})/L_{\mathrm{f}}^{\mathrm{SEV}}(x_{\mathrm{S}}, y_{\mathrm{S}}, t_{\mathrm{S}})$. Herefore, 6 quantities are estimated separately from SEVIRI Narrow-Band (NB) images (Clerbaux et al., submitted for publication-a, submitted for publication-b[I + II]):

- $L_{\mathrm{SW,sol}}^{\mathrm{SEV}}$, the dominating contribution of the reflected solar radiation to the SW radiance;
- $L_{\mathrm{SW,th}}^{\mathrm{SEV}}$, the small contribution of the emitted thermal radiation to the SW radiance;
- $L_{\mathrm{LW,th}}^{\mathrm{SEV}}$, the dominating contribution of the emitted thermal radiation to the LW radiance;
- $L_{\mathrm{LW,sol}}^{\mathrm{SEV}}$, the small contribution of the reflected solar radiation to the LW radiance;
- $L_{\mathrm{sol}}^{\mathrm{SEV}}$, the unfiltered reflected solar radiance estimate;
- $L_{\mathrm{th}}^{\mathrm{SEV}}$, the unfiltered emitted thermal radiance estimate.

These quantities are obtained as regression relations of the narrowband radiances trained on a database of simulated spectral distributions of synthetic scenes. The synthetic scenes are formed using atmospheric profiles from the TIGR-3 data base (Chevallier et al., 2000). The SBDART (Ricchiazi et al., 1998) radiative transfer tool is used.

The 'solar' quantities $L_{\mathrm{SW,sol}}^{\mathrm{SEV}}$ and $L_{\mathrm{LW,sol}}^{\mathrm{SEV}}$ are estimated from the solar SEVIRI radiances at 0.6, 0.8 and 1.6 μm. The 'thermal' quantities $L_{\mathrm{LW,th}}^{\mathrm{SEV}}$ and $L_{\mathrm{SW,th}}^{\mathrm{SEV}}$ are estimated from the thermal SEVIRI radiances at 6.2, 7.3, 8.7, 9.7, 10.8, 12.0 and 13.4 μm.

Filtered radiance estimates are obtained as:

$$\begin{aligned} L_{\mathrm{SW}}^{\mathrm{SEV}} &= L_{\mathrm{SW,sol}}^{\mathrm{SEV}} + L_{\mathrm{SW,th}}^{\mathrm{SEV}} \\ L_{\mathrm{LW}}^{\mathrm{SEV}} &= L_{\mathrm{LW,th}}^{\mathrm{SEV}} + L_{\mathrm{LW,sol}}^{\mathrm{SEV}} \end{aligned} \tag{6}$$

3.1.2. Angular modelling

The angular modelling consists in modelling the angular conversion factor $F^{\mathrm{SEV}}/L_{\mathrm{uf}}^{\mathrm{SEV}}$.

The LW angular modelling (Clerbaux et al., 2003) is based on plane parallel radiative transfer modelling using the same database of simulated scenes as used for the unfiltering. The thermal angular conversion factor $F_{\mathrm{th}}^{\mathrm{SEV}}/L_{\mathrm{th}}^{\mathrm{SEV}}$ is estimated as a function of the viewing zenith angle θ_{vz}, and as a function of the selected SEVIRI thermal radiances at 6.2, 10.8, 12.0 and 13.4 μm.

For the SW angular modelling, the ADM's derived from the CERES/VIRS combination on TRMM are used (Loeb et al., 2003). Cloud optical properties are derived from every SEVIRI pixel (Ipe et al., 2003, 2004), with resolution at nadir of 3 km, comparable with the determination of cloud optical properties from every VIRS pixel on TRMM, with resolution at nadir of 2 km. The ADM's are applied over windows of 3×3 SEVIRI pixels, which have a similar spatial resolution – around 10 km at nadir – as the CERES broadband radiometer on TRMM.

3.1.3. Main outputs

The outputs of this subsystem are SEVIRI based estimates of the GERB filtered radiances (SW and synthetic LW), the unfiltered radiances (reflected solar and emitted thermal), as well as the unfiltered broadband fluxes (reflected solar and emitted thermal) at 3×3 SEVIRI pixel resolution. Thus the outputs are images of $L_{\mathrm{f}}^{\mathrm{SEV}}$, $L_{\mathrm{uf}}^{\mathrm{SEV}}$ and F^{SEV}.

3.1.4. Auxiliary outputs

As auxiliary outputs, during daytime the cloud properties used for the SW ADM selection and aerosol properties over ocean (De Paepe et al., submitted for publication) are given. The cloud properties are:

- Cloud cover: relative number of cloudy pixels within a 3×3 SEVIRI pixel window;
- Cloud optical depth;
- Cloud phase.

Author's personal copy

The aerosol optical depths over ocean are given at the SEVIRI wavelengths of 0.6, 0.8 and 1.6 μm.

In this subsystem all the physical scene modelling is concentrated.

3.2. GERB Processing

In this subsystem, GERB broadband radiance measurements are combined with SEVIRI based models.

GERB is a broad band radiometer which makes images of the earth by scanning a North–South array of 256 detectors over the earth in East–West or West–East direction. TOTal images are taken by the blackened detectors, which are sensitive to both SW and LW radiation. SW images are obtained by inserting a quartz filter – rejecting radiation below 4 μm – in front of the detectors. TOT and SW images are obtained sequentially in time. One pair of SW and TOT images is obtained in 6 min. The resolution at nadir is approximatively 50 km.

The GERB detectors are calibrated in the Edition 1 NANRG GERB input product. For the spectral modelling and unfiltering an average TOT and SW spectral response is used for all detectors.

'(x_S, y_S, t_S)' is used to refer to SEVIRI time and space sampling, the spatial resolution is 3×3 SEVIRI pixels. '(x_G, y_G, t_G)' is used to refer to GERB time and space sampling.

The inputs for this subsystem are the images of the GERB TOT and SW radiances $L_f(x_G, y_G, t_G)$, the images of the SEVIRI based estimates of the SW and synthetic LW radiances $L_f^{SEV}(x_S, y_S, t_S)$, of the reflected solar and emitted thermal unfiltered radiances $L_{uf}^{SEV}(x_S, y_S, t_S)$ and of the fluxes $F^{SEV}(x_S, y_S, t_S)$.

3.2.1. Time interpolations

In the GERB Processing the calculations are done at the SW acquisition times and geolocations. GERB SW and TOT measurements are not taken at the same time and do not have exactly the same geolocation. The GERB TOT and the SEVIRI quantities are interpolated to SW acquisition times by linear interpolation between neighbouring measurements. After this step the SEVIRI quantities are available at SEVIRI spatial sampling and GERB times indicated as (x_S, y_S, t_G).

3.2.2. GERB footprint averaging

The SEVIRI quantities are averaged over the GERB footprint weighted with the GERB Point Spread Function (PSF). $PSF_{d,\lambda}(x - x_G, y - y_G)$ is the dynamical PSF for GERB detector d and wavelength-range λ which can be SW or LW. For example the GERB-like SW filtered radiance over the GERB footprint $L_{SW}^{SEV}(x_G, y_G, t_G)$ is obtained from the following equation

$$L_{SW}^{SEV}(x_G, y_G, t_G) = \int PSF_{d,SW}(x_S - x_G, y_S - y_G) L_{SW}^{SEV}(x_S, y_S, t_G) dx_S dy_S \quad (7)$$

3.2.3. Geolocation

The GERB geolocation is tuned to the SEVIRI geolocation by a matching process. A GERB geolocation model is used which allows to calculate the geolocation for every GERB pixel in function of geolocation parameters like the satellite position and attitude, and the satellite viewing angle parameters. The GERB geolocation parameters are varied iteratively such that a cost function quantifying the similarity between the GERB (with variable geolocation) and GERB-like (with fixed geolocation) filtered radiances is maximised.

The geolocation tuning is done separately for the GERB SW and TOT images.

3.2.4. Longwave calculation

The synthetic LW radiance is calculated by application of Eq. (2), after interpolation of the measured TOT radiances towards the GERB SW acquisition times and geolocations. The spatial interpolation from TOT to SW geolocation is done by triangular linear interpolation. The time interpolation is linear.

3.2.5. Line Of Sight (LOS) non repeatability correction

The pointing of a pixel of a GERB image of the earth in successive images of the earth is not rigorously constant due to jitter in the GERB pointing system. As a result the calculated LW radiances are contaminated by a SW gradient image. This SW contamination is not present in the GERB-like LW radiances, although these latter are radiometrically less accurate. The correction consists in smoothing the spectral correction factor, as indicated by the following equation

$$C(x_G, y_G, t_G) = L_{LW}(x_G, y_G, t_G) / L_{LW}^{SEV}(x_G, y_G, t_G)$$
$$L_{LW}^{corr}(x_G, y_G, t_G) = C^{corr}(x_G, y_G, t_G) L_{LW}^{SEV}(x_G, y_G, t_G) \quad (8)$$

$C^{corr}(x_G, y_G, t_G)$ is a spatially filtered version of $C(x_G, y_G, t_G)$. $C^{corr}(x_G, y_G, t_G)$ varies smoothly in space, hence the spatial structure of the corrected radiance $L_{LW}^{corr}(x_G, y_G, t_G)$ is the one of the GERB-like (SEVIRI based) $L_{LW}^{SEV}(x_G, y_G, t_G)$, and it does not contain the SW contamination. $C^{corr}(x_G, y_G, t_G)$ has the same average level as $C(x_G, y_G, t_G)$, hence the corrected radiance $L_{LW}^{corr}(x_G, y_G, t_G)$ has the same radiometric level as the uncorrected radiance $L_{LW}(x_G, y_G, t_G)$.

3.2.6. Unfiltering and angular conversion

The SEVIRI quantities $L_f^{SEV}(x_S, y_S, t_S)$, $L_{uf}^{SEV}(x_S, y_S, t_S)$ and $F^{SEV}(x_S, y_S, t_S)$ are interpolated and averaged over the GERB SW footprints towards $L_f^{SEV}(x_G, y_G, t_G)$, $L_{uf}^{SEV}(x_G, y_G, t_G)$ and $F^{SEV}(x_G, y_G, t_G)$. The LW and SW spectral correction factors are evaluated over the GERB

Author's personal copy

footprints $C(x_G, y_G, t_G) = L_f(x_G, y_G, t_G)/L_f^{SEV}(x_G, y_G, t_G)$. The unfiltered radiances $L_{uf}(x_G, y_G, t_G)$ and fluxes $F^{SEV}(x_G, y_G, t_G)$ are evaluated by application of Eqs. (4) and (5) over the GERB footprints. The outputs form the GERB 6′ products.

3.2.7. ARG averaging

The radiometric quantities L^f, L^{uf}, F are rectified to a common grid and averaged over three consecutive GERB images to form the ARG product. The correction factor C is calculated based on the averaged quantities and is provided as a quality indicator. For the LW case the correction factor with and without the LOS non repeatability correction are given.

In this subsystem all the GERB–SEVIRI coregistration and the GERB radiometric processing is concentrated.

3.3. Resolution enhancement

In this subsystem, the resolution of the GERB 6′ fluxes is improved by use of SEVIRI high resolution information. The resolution enhancement is the inverse operation of the resolution degradation by weighting over the GERB PSF as in Eq. (7). Spectral correction factors are defined at low $C(x_G, y_G, t_G)$ and high resolution $C(x_S, y_S, t_G)$. The high resolution correction factors are determined by imposing two conditions:

- Integration of $C(x_S, y_S, t_G)L_f^{SEV}(x_S, y_S, t_G)$ over the GERB footprint reproduces $C(x_G, y_G, t_G)L_f^{SEV}(x_G, y_G, t_G)$;
- The spatial variation of $C(x_S, y_S, t_G)$ is as smooth as possible.

These conditions are met approximately by the iterative minimisation of an appropriate cost function. More details are given in Gonzalez et al. (2000).

3.3.1. SHI averaging

The SHI product is a 15′ snapshot at high resolution (x_S, y_S, t_S). In order not to introduce artefacts due to moving clouds no averaging of the radiometric quantities L^f, L^{uf}, F is performed. Instead 15 min means $C(x_S, y_S, t_S)$ centered around the SEVIRI acquisition time of the spectral correction factors $C(x_S, y_S, t_G)$ are calculated. The unfiltered radiances and fluxes are calculated by application of Eqs. 4 and 5 using the mean spectral correction factors $C(x_S, y_S, t_S)$.

3.3.2. BARG averaging

The radiometric quantities L^f, L^{uf}, F are averaged over 5×5 3×3 SEVIRI pixels, and over 15′ time intervals synchronised to UTC (first interval: 00:00–00:15 UTC). The 15′ time integration assumes a piecewise linear variation in between GERB SW measurement times. The correction factor C is calculated based on the averaged quantities and is provided as a quality indicator. For the LW case the correction factor with and without the LOS non repeatability correction are given. In this subsystem all the resolution enhancement of GERB by SEVIRI is concentrated.

3.4. Data versions

The GERB 2 data is processed in near-real time. The current near-real time products are labelled 'Version 3' and are available for scientific usage after registration at http://gerb.oma.be. Version 3 exists for the ARG,SHI and BARG products. After a 40 day quality control period the ARG V3 is relabelled 'Edition 1' and is transferred to a long term archive accessible through http://ggsps.rl.ac.uk/.

4. Summary validation results

The accuracy of the Edition 1 GERB unfiltered radiances and fluxes – which are presented in this paper – depends on a multitude of parameters. The basic GERB measurements are the GERB filtered radiances, whose accuracy depends on the on-ground and in-flight calibration (Harries, 2004). An important source of uncertainty is the limited knowledge of the spectral response, which has an influence both on the calibration and on the unfiltering. Uncertainties in the geolocation determine how well GERB and SEVIRI can be matched and hence they have an influence on the unfiltering, angular conversion and resolution enhancement.

In order to get an overall estimate of the GERB accuracy, the GERB products can be compared with the independent CERES products. The CERES radiometers measure the same quantities as the GERB radiometer – unfiltered broadband radiances and fluxes – from low earth orbit satellites.

We have compared GERB ARG Edition 1 and SHI and BARG Version 3 data with CERES ES8 Edition 1 Revision 1 with in-flight gain changes. We have used the three active CERES instruments FM1, FM2 (both on the Terra satellite) and FM3 (on the Aqua satellite). All results presented are mean values over the period from 25 March to 30 April 2006.

The CERES measurements are mapped to the GERB footprints which are closest in time, with a maximum time difference of 7.5 min. All CERES measurements falling in the same GERB footprint are averaged.

The comparison of co-angular co-located unfiltered radiances allows to check the basic calibration and spectral unfiltering. For the radiance comparison we only retain CERES radiances that are co-angular with the GERB ones within 20°. Table 1 shows the average GERB/CERES ratios for the 3 GERB product types (ARG, SHI, BARG), for the 3 CERES instruments, for the SW radiances, and for the LW radiances during night and during day.

For the day time comparisons, there are about 150,000 GERB–CERES radiance matches per CERES instrument, for the night time comparisons, there are about 50,000 GERB–CERES radiance matches per CERES instrument.

Author's personal copy

Table 1
Co-angular, unfiltered GERB/(CERES ES-8) radiance ratios for the time period from 25 March to 30 April 2006

Radiance	Solar			Thermal night			Thermal day		
GERB/CERES	FM1	FM2	FM3	FM1	FM2	FM3	FM1	FM2	FM3
ARG	1.038	1.046	1.056	0.981	0.989	0.987	0.987	0.964	0.978
SHI	1.047	1.055	1.063	0.965	0.973	0.979	0.978	0.956	0.967
BARG	1.036	1.044	1.057	0.977	0.984	0.989	0.987	0.963	0.978

Rows: ratios for GERB ARG, SHI and BARG products. First 3 columns: reflected solar radiance ratio for the three CERES instruments (FM1, FM2, FM3). Next 3 columns: night time thermal radiance ratio for the three CERES instruments. Final 3 columns: day time thermal radiance ratio for the three CERES instruments.

The ARG and BARG ratios agree within a fraction of a percent, validating the spatial transformations in the resolution enhancement and the ARG and BARG averaging.

Compared to the ARG and BARG ratio, the SHI ratio is systematically higher in the SW (by almost 1%) and lower in the LW (by almost 1%). This can be explained by the different type of time averaging used in the SHI (averaging of spectral correction factors C) and the ARG and BARG (averaging of radiances and fluxes).

As different scene types have different spectral behaviour, differences in calibration and spectral unfiltering can be differentiated by making a radiance comparison per scene type. Table 2 shows the average GERB/CERES ratios for the GERB ARG product, for the 3 CERES instruments, for the following scenes: clear sky ocean, dark vegetation, bright vegetation, dark desert and bright desert, thin, medium and thick clouds. The surface scene types are the ones used in the CERES ADM definition, the cloudiness classes are defined based on cloud optical depth τ, clear sky: $\tau < 1$, thin clouds: $1 < \tau < 3.16$, medium clouds: $3.16 < \tau < 10$, thick clouds: $\tau > 10$.

The target accuracy for both GERB and CERES reflected solar radiances is 1%, thus the maximum differences should be 2%. For thick clouds, the difference with FM1 of 1.3% is within this maximum difference, and the difference with FM2 and FM3 of 2.3% is close. For the other scene types GERB is significantly higher, with a maximum difference between clear sky ocean and thick clouds of 6.4%. The scene type dependency of the GERB/CERES reflected solar ratio is probably due to the imperfect knowledge of the GERB 2 spectral response $\Phi_{SW}(\lambda)$ which influences the SW unfilter factor α_{uf}.

At night – when there is no problem of thermal solar separation – the ARG and BARG LW radiance are 1–2% lower than CERES.

The difference between day and night LW ratios varies with CERES instrument, there is an agreement within 1% with FM1 and FM3, validating the thermal separation.

In addition to radiance comparisons, the comparison of non co-angular co-located fluxes allows to check the angular conversion depending on the scene identification. Table 3 shows the average GERB/(CERES ES-8) reflected solar flux ratios per scene type and per CERES instrument. The CERES ES-8 uses the ERBE-like scene identification and hence does not use the most advanced CERES ADM's. The ratios are similar to those of the radiances

Table 2
Scene type dependency for co-angular co-located GERB ARG/(CERES ES-8) reflected solar radiance ratios for the time period from 25 March to 30 April 2006

ARG Sol. Rad.	Clear					Thin	Medium	Thick
GERB/CERES	Ocean	D. Veg.	B. Veg.	D. Des.	B. Des.			
FM1	1.077	1.056	1.061	1.061	1.046	1.044	1.031	1.013
FM2	1.086	1.060	1.064	1.064	1.046	1.052	1.039	1.023
FM3	1.069	1.080	1.062	1.070	1.070	1.064	1.057	1.023

Rows: ratios for three CERES instruments (FM1, FM2, FM3). First 5 columns: ratio for clear sky surfaces: Ocean, D. Veg., dark vegetation; B. Veg., bright vegetation; D. Des., dark desert; B. Des., bright desert. Final 3 columns: ratios for varying cloud optical depths τ: thin: $1 < \tau < 3.16$, medium: $3.16 < \tau < 10$, thick: $\tau > 10$. Clear sky is identified by $\tau < 1$.

Table 3
Co-located GERB ARG/(CERES ES-8) reflected solar flux ratios for the time period from 25 March to 30 April 2006

ARG Sol. Flux	Clear					Thin	Medium	Thick
GERB/CERES	Ocean	D. Veg.	B. Veg.	D. Des.	B. Des.			
FM1	1.120	1.004	1.061	1.069	1.065	1.064	1.029	1.017
FM2	1.117	1.007	1.065	1.070	1.067	1.069	1.036	1.025
FM3	1.120	1.009	1.069	1.073	1.076	1.078	1.053	1.035

Rows: ratios for three CERES instruments (FM1, FM2, FM3). First 5 columns: ratio for clear sky surfaces: Ocean, D. Veg., dark vegetation; B. Veg., bright vegetation; D. Des., dark desert; B. Des., bright desert. Final 3 columns: Ratios for varying cloud optical depths τ: thin: $1 < \tau < 3.16$, medium: $3.16 < \tau < 10$, thick: $\tau > 10$. Clear sky is identified by $\tau < 1$.

Author's personal copy

except for clear sky ocean and clear sky dark vegetation. The reflected solar angular conversion factor α_{adm} is 3–5% too high for ocean and 5–6% too low for dark vegetation.

The comparison of the thermal fluxes reveals a regional overestimation for near nadir observations and a regional underestimation for near limb observations of cold cloud and hot desert scenes. It was decided not to correct this effect in Edition 1 GERB 2 fluxes in order to keep the GERB and the CERES instruments independent of each other. If an individual user wants to use the fluxes for regional studies close to nadir or to the limb, the following correction on the thermal flux F_{th} is advised:

$$\begin{aligned}&\text{if } F_{\mathrm{th}} \leqslant 322\ \mathrm{W/m^2}:\\ &\mathrm{ne} = -0.023 - 0.0015 * F_{\mathrm{th}} + 4.5e-05 * F_{\mathrm{th}}^2\\ &\qquad - 2.5e-07 * F_{\mathrm{th}}^3 + 3.93e-10 * F_{\mathrm{th}}^4 \qquad (9)\\ &\text{else}:\\ &\mathrm{ne} = -2.885 + 0.02036 * F_{\mathrm{th}} - 4.57e-05 * F_{\mathrm{th}}^2\\ &\qquad + 3.31e-08 * F_{\mathrm{th}}^3\\ &F_{\mathrm{th}}^{\mathrm{corr}} = F_{\mathrm{th}} \Big/ \left(1 + \mathrm{ne}\left(1 - \frac{\theta_{\mathrm{vz}}}{52.5^\circ}\right)\right) \qquad (10)\end{aligned}$$

F_{th} is the uncorrected Edition 1 GERB 2 thermal flux, θ_{vz} is the viewing zenith angle in degrees, $F_{\mathrm{th}}^{\mathrm{corr}}$ is the corrected thermal flux.

5. Conclusions

The GERB 2 instrument on Meteosat 8 is the first instrument to measure the regional radiation budget from a geostationary orbit, with an unprecedented time resolution of 6 min. In this paper we have presented an overview of the processing of the basic GERB measurements – filtered broadband radiances – towards the user products of the radiative energy fluxes of reflected solar radiation and emitted thermal radiation. The multispectral imager SEVIRI on the same satellite is used for the modelling of spectral and angular distribution of the radiation, as well as to increase the resolution of the GERB measurements.

The GERB products are provided in different time-space sampling, the ARG is the basic 45 km 17 min average of three GERB measurements, the SHI is a high resolution 9 km 15 min product, and the BARG is a binned 45 km 15 min product. The three products are produced in near-real time as Version 3, and are available from http://gerb.oma.be. The ARG product is transferred to a long term archive after manual quality control as Edition 1, and is available from http://ggsps.rl.ac.uk/.

The GERB products have been compared with the independent CERES ES8 for validation. Limits of the accuracy of the GERB 2 Edition 1 products are the knowledge of the GERB SW spectral response, the reflected solar angular conversion for clear sky ocean and clear sky dark vegetation, and the regional error of the emitted thermal angular conversion for cold clouds and hot desert. For the latter an empirical correction is advised. Overall, there is GERB–CERES agreement within 5% for the reflected solar radiances and within 2% for the emitted thermal radiances. For the reflected solar radiances, the best relative agreement is reached for thick clouds and the worst relative agreement is reached for clear sky ocean. For the reflected solar fluxes, the angular conversion factor is too high for clear sky ocean and is too low for clear sky dark vegetation.

References

Barkstrom, B.R.ERBE Science Team The Earth Radiation Budget Experiment (ERBE). Bulletin of the American Meteorological Society 65, 1170–1186, 1984.

Chevallier, F., Chedin, A., Chéruy, F., Morcrette, J.J. TIGR-like atmospheric-profile databases for accurate radiative-flux computation. Quarterly Journal of the Royal Meteorological Society 126, 777–785, 2000.

Clerbaux, N., Dewitte, S., Gonzalez, L., Bertrand, C., Nicula, B., Ipe, A. Outgoing longwave flux estimation: improvement of angular modelling using spectral information. Remote Sensing of Environment 85, 389–395, 2003.

Clerbaux, N., Dewitte, S., Bertrand, C., Caprion, D., Depaepe, B., Gonzalez, L., Ipe, A., Russell, J. Unfiltering of the Geostationary Earth Radiation Budget (GERB) data. Part I. Shortwave Radiation, Journal of Applied Meteorology, submitted for publication-a.

Clerbaux, N., Dewitte, S., Bertrand, C., Caprion, D., Depaepe, B., Gonzalez, L., Ipe, A., Russell, J. Unfiltering of the Geostationary Earth Radiation Budget (GERB) data. Part II. Longwave Radiation, Journal of Applied Meteorology, submitted for publication-b.

B. De Paepe, A. Ignatov, S. Dewitte, A. Ipe. The GERB aerosol product: cloud screening and validation, Remote Sensing of Environment, submitted for publication.

Gonzalez, L., Hermans, A., Dewitte, S., Ipe, A., Sadowski, G., Clerbaux, N. Resolution enhancement of GERB data, in: Proceedings of the 2000 EUMETSAT Meteorological Satellite Data Users' Conference, pp. 619–625, 2000.

Harries, J., Russell, J., Hanafin, J., Brindley, H., et al. The Geostationary Earth Radiation Budget Project. Bulletin of the American Meteorological Society 86 (7), 945–960, 2004.

Ipe, A., Clerbaux, N., Bertrand, C., Dewitte, S., Gonzalez, L. Pixel-scale composite top-of-the-atmosphere clear-sky reflectances for Meteosat-7 visible data. Journal of Geophysical Research 108 (D19), 4612, 2003.

Ipe, A., Bertrand, C., Clerbaux, N., Dewitte, S., Gonzalez, L. Validation and homogenisation of cloud optical depth and cloud fraction retrievals for GERB/SEVIRI scene identification using Meteosat-7 data. Atmospheric Research 72, 17–37, 2004.

Kandel, R., Viollier, M., Pakhomov, L.A., Golovko, V.A., Raschke, E., Stuhlmann, R. The ScaRaB earth radiation budget dataset. Bulletin of the American Meteorological Society 79, 765–783, 1998.

Loeb, N., Manalo-Smith, N., Kato, S., Gupta, S.K., Minnis, P., Wielicki, B. Angular distribution models for top-of-atmosphere radiative flux estimation from the Clouds and the Earth's Radiant Energy System instrument on the Tropical Rainfall Measuring Mission satellite. Journal of Applied Meteorology 42, 1748–1769, 2003.

Ricchiazi, P., Yang, S., Gautier, C., Sowle, D. SBDART: a research and teaching software tool for plane-parallel radiative transfer in the earth's atmosphere, 79, pp. 2101–2114, 1998.

Schmetz, J., Pili, P., Tjemkes, S., Just, D., Kerkmann, J., Rota, S., Ratier, A. An introduction to Meteosat Second Generation (MSG). Bulletin of the American Meteorological Society 83, 977–992, 2002.

Wielicki, B., Barkstrom, B.R., Harrison, E.F., Lee III., R.B., Smith, G.L. Clouds and the Earth's Radiant Energy System (CERES): an Earth Observing System experiment. Bulletin of the American Meteorological Society 77, 853–868, 1996.